Volume 26
Number 10
21 May 2024
Pages 5585-6220

Green Chemistry

Cutting-edge research for a greener sustainable future

rsc.li/greenchem

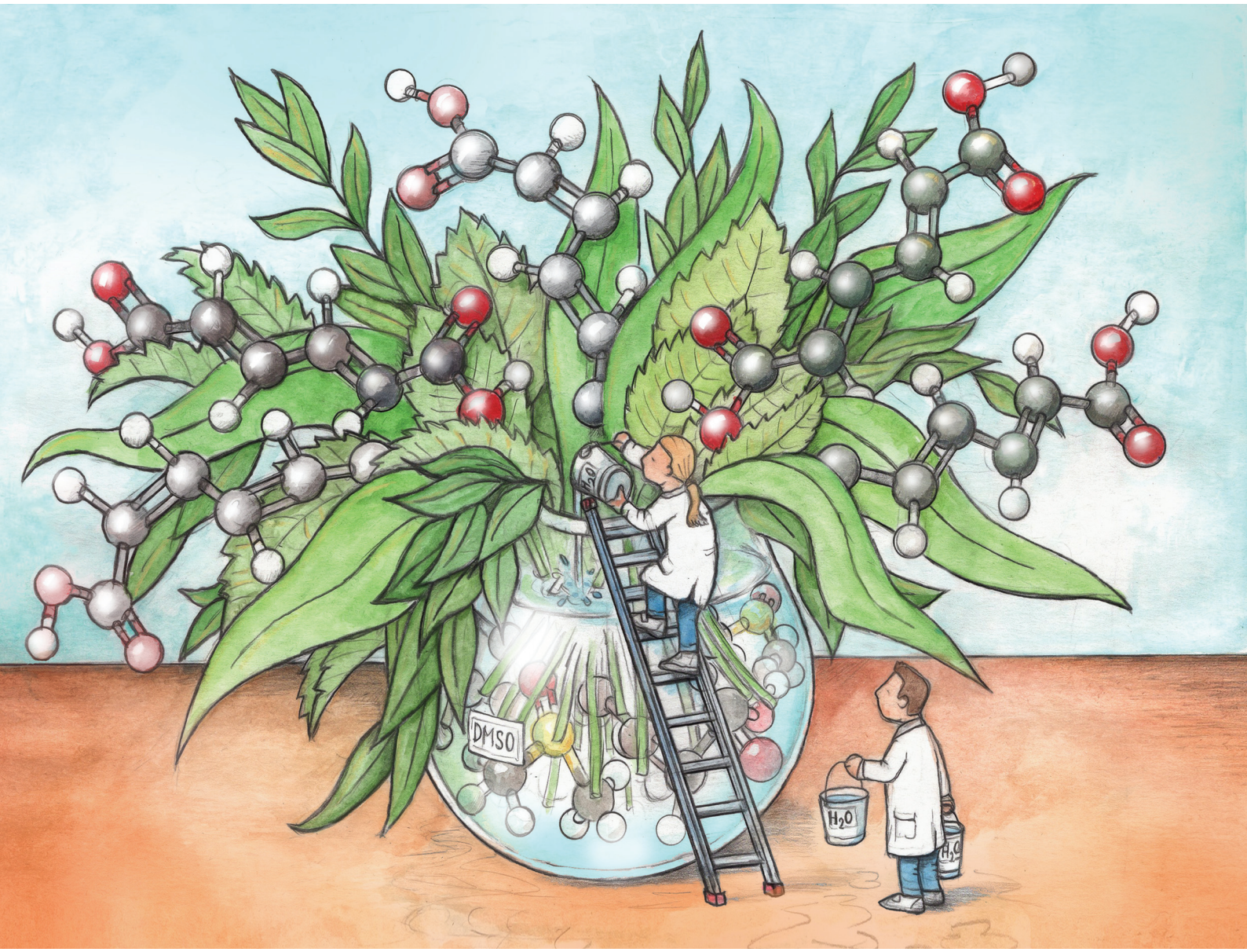

ISSN 1463-9262

ROYAL SOCIETY OF CHEMISTRY

PAPER

Ibrahim Khalil, Michiel Dusselier *et al.*
Solvent-driven isomerization of muconates in DMSO: reaction mechanism and process sustainability

25 YEARS ANNIVERSARY

Green Chemistry

PAPER

View Article Online
View Journal | View Issue

Cite this: *Green Chem.*, 2024, **26**, 5852

Solvent-driven isomerization of muconates in DMSO: reaction mechanism and process sustainability†

Ibrahim Khalil, *[a] Fatima Rammal, [a] Lisa De Vriendt, [a] An Sofie Narmon, [a] Bert F. Sels, [a] Sebastian Meier [b] and Michiel Dusselier *[a]

The production of renewable chemicals and monomers is fundamental for transitioning to a future circular economy. Currently, *cis*,*cis*-muconic acid (*cc*MA) is a bio-sourced platform chemical with great potential for added-value chemicals, monomers, and specialty polymers. Among the three isomers, the *trans*, *trans* (*tt*-isomer) stands out due to its reactivity for polymerization and unique ability as a substrate for the Diels–Alder cycloaddition reaction. Whereas earlier research has focused on producing this isomer, the most promising solvent-driven isomerization in DMSO-containing water yields moderate *tt*MA due to a competitive ring-closing lactonization reaction, especially in highly concentrated systems. This work highlights the unique ability of DMSO, among several other solvents, to produce *tt*MA. In addition, we report the effect of the acidity of the initial MA concentration and the amount of water on the lactonization reaction. Control of reaction conditions and use of muconates (diethyl muconates = DEM) countered the competitive lactonization, reaching >90% *tt*-isomer selectivity. The involvement of water and DMSO in the isomerization mechanism was investigated in detail by probing the reaction mechanism with *in situ* NMR. Identifying the reaction products and several intermediates led us to propose a plausible mechanism. Based on this knowledge, condition optimization led to a significant thirty-fold *tt*DEM productivity improvement, *viz.* from 10 to 328 mM h^{-1}. The DEM can be isolated almost quantitatively from the DMSO solvent system by extraction.

Received 23rd January 2024,
Accepted 25th March 2024

DOI: 10.1039/d4gc00395k

rsc.li/greenchem

Introduction

The migration from a petroleum-based chemical industry can be assisted by the development of processes that produce and convert platform molecules derived from renewable carbon sources.[1–5] Biomass serves as one of the most promising renewable sources for high-value chemicals.[6–10] An example of such a high-value chemical is 2,4-hexenedioic acid, known as muconic acid (MA).[11,12] Due to its conjugated double bonds and carboxyl groups at both ends, MA serves as a precursor for valuable monomers, such as adipic acid (AA), ε-caprolactam, and terephthalic acid (TPA).[13–15] It is also used to prepare the novel hexenedioic acid (HDA) and cyclohexane-1,4-dicarboxylic acid (CHDA) monomers.[15–17] These monomers are mainly used for the production of polyamides (PA), polyesters, and polyurethanes.[18–20] Note that MA itself can be used as a monomer for homo- and co-polymerization reactions.[15,21]

MA is present in three geometric isomeric forms, two of which can be obtained from bio-based sources: *cis*,*cis*-MA and *cis*,*trans*-MA (*cc*MA and *ct*MA).[17,22–25] *ct*MA can also be obtained from the spontaneous isomerization of *cc*MA under acidic conditions.[15,26] However, the preferred isomer for polymerization and certain chemical transformations (*e.g.*, Diels–Alder cycloaddition), *trans*,*trans*-MA (*tt*MA), can only be obtained chemically by synthesis or isomerization.[12,26,27] The most prominent catalytic isomerization protocol for the production of *tt*MA and muconates (muconic esters) is the homogenous I_2 catalyzed isomerization,[28,29] besides two heterogeneously catalyzed methods using 5%Pd/C and Ru-hydride/zeolite (0.2%Ru) have been developed.[30,31] Research on non-catalytic isomerization routes showed that dimethyl sulfoxide (DMSO) could promote the formation of *tt*MA from *ct*MA, albeit at moderate yield and in low concentrated solutions.[26] Other solvents, such as triethylamine, toluene, acetone, acetonitrile, 2-propanol, methanol, hexanol, tetrahydrofuran, and ethyl acetate, showed no isomerization activity. The main side

[a]*Center for Sustainable Catalysis and Engineering (CSCE), KU Leuven, Celestijnenlaan 200F, B-3001 Leuven, Belgium. E-mail: khalil.ibrahim@kuleuven.be, michiel.dusselier@kuleuven.be*
[b]*Department of Chemistry, Technical University of Denmark, Kemitorvet 207, 2800 Kgs. Lyngby, Denmark*

† Electronic supplementary information (ESI) available. See DOI: https://doi.org/10.1039/d4gc00395k

product observed in all solvents was mono-muconolactone (Mlac), as a result of a competitive irreversible intramolecular lactonization, in essence, a ring closing of MA.[15,26,32] This reaction can be reduced, providing higher *tt*MA yields, by controlling the water amounts in DMSO.[32] The role of water was only effective until a concentration of 0.5 M, yielding 39% *tt*MA at 50% *ct*MA conversion. Above this concentration, the DMSO-driven system suffers from low yields and selectivity, where at 2 M concentration, *tt*MA was hardly formed with <1% yield at 50% conversion.[32] Besides the moderate results, the mechanism of DMSO-driven isomerization is not fully understood, therefore missing handles to improve *tt*MA yields in concentrated solutions.

In this work, we first investigated the isomerization of *cc*MA into *ct*MA in various solvents (including DMSO), where the lactones formation was also followed experimentally as a function of the concentration of MA and the used solvent. We effectively countered the competitive lactonization by protecting the carboxylic groups by esterification. Additionally, the dynamics of isomerization of both MA and muconates were followed with *in situ* NMR measurements. Although we find that the role of water was less pronounced when using muconates, its presence was always required for high *tt*-isomer production. Further, careful identification and real-time tracking of intermediates and their byproducts clarified the role of DMSO in the isomerization mechanism. This insight led us to achieve outstanding process isomerization efficiency, outperforming known catalyst-free MA isomerizations. As opposed to current systems, we can isomerize >0.5 M muconates solutions in high productivity and selectivity > 95%. The recovery of the DEM isomers from DMSO was successfully performed, with recovery levels surpassing 90%.

Experimental

Materials

cis,*cis*-Muconic acid (*cc*MA) was purchased from Fluorochem with a purity >99%. Ethanol (99.8%) and anhydrous magnesium sulfate $MgSO_4$ were supplied by Fisher. Ethyl acetate (99.5%), DMSO (99.5%), acetonitrile (99.9%), *N*,*N*-dimethylformamide (DMF) (>99%), acetone (>99%), toluene (99.5%), and 96% sulfuric acid in water H_2SO_4/H_2O were supplied by Acros. Sodium chloride (>99.5%) was supplied by Carl Roth. Anhydrous DMSO (99.9%), triethylamine (>99.5%), and the 9 mL glass pressure tubes were supplied from Merck. The length of the glass pressure tubes was optionally reduced (10.2 to around 6 cm) at a glassblower workshop for performing low-volume reactions (1–2 mL).

Preparation of *ct*MA and *ct*DEM

***cc*MA to *cis*,*trans*-MA (*ct*MA).** *ct*MA was formed by isomerization of 2.0 g of *cc*MA in 100 ml deionized water at 80 °C for 75–80 minutes. After the reaction, the solution was cooled to room temperature, and crystals of pure *ct*MA started to form. After 18 hours (overnight), *ct*MA crystals were filtrated and dried at 60 °C under air to recover 1.4 ± 0.1 g. Optionally, the recovery level can be improved by partially removing water under reduced pressure, more *ct*MA will precipitate. After filtration and air drying at 60 °C, an additional 0.2 ± 0.05 g of pure *ct*MA were collected. The total recovery yield was around 72–88%.

Esterification of *ct*MA to *ct*DEM. The esterification of *ct*MA into *ct*-diethylmuconate (*ct*DEM) was performed following our previously reported procedure. 2.0 g of *ct*MA were added in 100 mL ethanol containing a few drops of aqueous sulfuric acid solution (H_2SO_4/H_2O). The solution was brought to reflux for 24 hours. After cooling, ethanol was removed under reduced pressure (rotary evaporator), and the remaining liquid was extracted with ethyl acetate (EtOAc). The organic phase was dried over $MgSO_4$ and the solvent was removed under reduced pressure to obtain pure *ct*DEM with a 90–95% isolated yield.

The reaction conditions for the isomerization (towards *tt*-isomer and Mlac products)

The formation of *tt*-isomer from the *ct*-form was performed in 9 mL pressure tubes (or modified pressure tubes with a total volume of 6 mL). Solutions of 3–5 mL of different solvents (H_2O, ethanol, acetonitrile, DMSO, DMF, acetone, triethylamine, or toluene) containing *cc*MA, *ct*MA, or *ct*DEM in a concentration range from 30 to 3200 mM were prepared. Optionally, other solvents and substrates were added to the mixture such as H_2O, $DMSO_2$, sulfolane, and methylphenyl sulfoxide. For the experiments with dry DMSO, a commercial anhydrous DMSO was used, where the liquid was extracted under a flow of argon. After filling all the components, the glass pressure tube was sealed at room temperature, and reactions were conducted at the desired temperature (a range of 80 to 150 °C was investigated) in an oil bath. The conversion and product distribution were determined using ^{1}H-NMR and $DMSO_2$ as an external standard for the experiments studying the isomerization of MA. For analyzing the isomerization results of DEM, gas phase chromatography (GC) was used with *n*-heptane as an external standard.

Recovery of *ct*DEM and *tt*DEM from DMSO

The mixture containing DEM isomers (*ct*DEM and *tt*DEM) was extracted from DMSO by first dissolving 10 mL of the reaction mixture in 10 mL of distilled water. 5 mL of EtOAc was then added, and *tt*DEM and *ct*DEM were extracted after vigorous stirring, followed by degassing.[33] This step was repeated three times to collect 15 mL EtOAc phase, which was then washed with brine, dried over $MgSO_4$, filtered, and concentrated under reduced pressure. The recovery level *r* was calculated as:

$$r = [\mathrm{DEM}]_{\mathrm{EtOAc}}/[\mathrm{DEM}]_{\mathrm{initial}}.$$

Analysis methods

^{1}H-NMR. ^{1}H-NMR spectra were recorded on a Bruker Avance 400 MHz spectrometer with a BBI 5 mm probe. DMSO-d_6 (Sigma-Aldrich) solvent was used as a solvent, and $DMSO_2$ was

used as an external standard. D_2O was not selected to avoid possible changes in chemical shifts related to different pH values but also due to the very limited solubility of *tt*MA in water (<0.1 g L^{-1}).[15] The ^{1}H-NMR spectra and the chemical shifts of the MA (*cc*MA, *ct*MA, and *tt*MA) and muconate (*ct*DEM) isomers can be found in our work.[31]

Gas phase chromatography (GC). The product distribution from the isomerization reactions of DEM was estimated using an Agilent Technologies 6890 N gas chromatograph equipped with a DB-17 capillary column of 0.32 mm of internal diameter and N_2 as carrier gas. Of the solution, 0.2 μL was injected at 250 °C with a split ratio of 25 : 1. The gas mixture was further driven to the column (initially at 80 °C) with a flow of 2.6 mL min^{-1}. After 5 min at 80 °C, the temperature was increased to 200 °C (10 °C min^{-1}) and held for 3 min, and then to 280 °C (20 °C min^{-1}) and held there for 6 min. The FID detector used was maintained at 320 °C. *n*-Heptane was used as an external standard. The calibration curve was derived, yielding a response ratio for *ct*DEM of $A_{ctDEM}/A_{heptane}$ = 1.408 [*ct*DEM]/[heptane]. The same response factor was used for the quantification of *tt*DEM.

All the quantified products were identified based on retention times, using pure components or mixtures with various ratios as references, with the relevant retention times being *n*-heptane (~1.5 min)/*tt*DEM (~15.0 min)/*ct*DEM (~15.3 min).

pH readings method. The pH reading was performed using a digital pH meter (Mettler Toledo) equipped with a Pro-ISM pH sensor. A calibration was first performed using four solutions with varied pH values (4.01, 7.00, 9.21, and 11.00). 5 mL of DMSO were filled into a 12 mL glass vial and the pH sensor was immersed in the solution. After adding the substrates, the solution was stirred until homogenization, and the pH was measured. Since organic solvents are usually ion deficient, pH readings were often unstable and, therefore, require a longer time to stabilize.

Real-time kinetic ^{1}H-NMR assays and advanced 2D NMR identification of diagnostic side products. Real-time observations of isomerization reactions were conducted using DMSO-d_6 as the lock substance on an 800 MHz Bruker Avance III instrument equipped with a 5 mm TCI cryoprobe and an Oxford magnet (18.7 T), or on a 600 MHz Bruker Avance III instrument equipped with a 5 mm BBO Smart probe.

Time series of ^{1}H-NMR spectra (using the zgcppr pulse sequence) were acquired by accumulating 64 transients with an interscan relaxation delay of 3 seconds and sampling the FID for 1.7 s (16 384 complex data points), yielding a time resolution of 5 min per spectrum. All real-time kinetic NMR tracking was implemented in the form of pseudo-2D experiments. With these experiments, the conversion of MA acids and esters was tracked at the indicated temperatures, and approximately 250 time points were acquired in the pseudo-2D experiments. The kinetic data were processed using zero filling to 32 768 complex data points and an exponential window function with 3 Hz line broadening (LB) in Bruker Topspin 4.1.3. Reaction progress data from the pseudo-2D experiments were integrated in the same software. Signal areas were plotted using software pro Fit 7 (QuantumSoft).

Products in post-reaction mixtures were identified at 25 °C using a suite of homo- and heteronuclear 2D NMR assignment spectra including ^{1}H–^{1}H COSY, ^{1}H–^{1}H TOCSY, ^{1}H–^{13}C HSQC, ^{1}H–^{13}C HSQC-TOCSY and ^{1}H–^{13}C HMBC spectra to annotate the assignments, provided herein.

Assignment spectra were acquired using Topspin 3.5 pl6. These spectra were processed with zero filling to at least twice the number of acquired complex data points in Bruker Topspin 4.1.3, and analyzed in the same software.

Results and discussion

Isomerization *vs.* lactonization of muconic acid: solvent dependency

The first isomerization of *cc*MA to *ct*MA is known to occur under conditions as mild as 25 °C in water. However, this isomerization step is pH-dependent and should preferentially be performed at a pH below 4. The isomerization is also temperature-dependent, and can be accelerated from a few days to less than an hour by increasing the temperature from 25 to 75 °C.[18,26,34,35] Fig. S1† summarizes the isomerization products obtained over the course of 4 hours for a solution of 30 mM *cc*MA in water at 75 °C. The complete conversion of *cc*MA occurs within 40 minutes, leading to *ct*MA initially, but just before *cc*MA conversion is complete, Mlac starts to be generated due to the intramolecular lactonization of the *ct*MA intermediate. This reaction is known to be assisted by water, as previously reported by Tessonnier *et al.* (Fig. S2 and S3†).[26] To investigate the solvent effect on the isomerization of *cc*MA and the competitive lactonization towards Mlac, we studied the reaction in a selection of solvents with different polarity and proticity, namely water, ethanol, acetone, toluene, acetonitrile (MeCN), *N*,*N*-dimethylformamide (DMF), triethylamine (Et_3N), and dimethyl sulfoxide (DMSO) (Fig. S4†). The reactions were conducted at 90 °C for 4 hours (30 mM *cc*MA), and the results are presented in Fig. 1.

A good carbon balance was observed overall (80–98%) except for Et_3N, in which the degradation of MA was noticed. The degradation may be linked to the basic nature of Et_3N since, correspondingly, partial loss in the carbon balance was also noticed when using MeCN, which shares basic characteristics. In addition to the basicity, the polarity of the solvents seems to influence the conversion of *cc*MA, since minimal conversion (1 to 5%) was noticed in acetone, cycloalkanes, alkanes, and toluene (least polar solvents in our range) in comparison to complete conversion in H_2O (polar) and DMF (basic nature and semi-polar). We note that the solubility of *cc*MA in the least polar solvents was very limited. EtOH and DMSO afforded partial conversion of *cc*MA with 70% and 90%, respectively. For EtOH, the high conversion of *cc*MA can be due to its protic properties next to its polarity. Interestingly, when testing alcohols with longer alkyl chains (1-butanol, 1-hexanol, and 1-octanol), we notice a decrease in the *cc*MA isomerization, which is due to the decrease in the proticity of the alcohols (less acidic proton) when the size of the alkyl

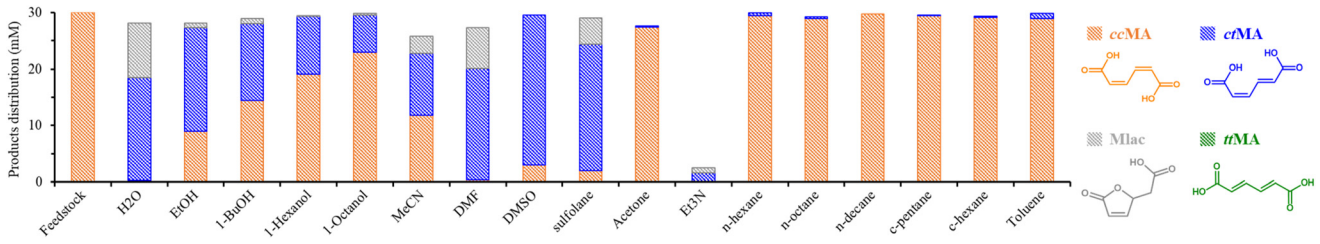

Fig. 1 The product distribution (in mM) for the conversion of 30 mM *cc*MA into *ct*MA and mono-muconolactone (Mlac) in various solvents (3 mL) at 90 °C for 4 hours. The reaction was performed in a glass pressure tube sealed under static conditions at room temperature. Abbreviations for solvents: EtOH = ethanol, 1-BuOH = 1-butanol, MeCN = acetonitrile, DMF = *N*,*N*-dimethylformamide, DMSO = dimethyl sulfoxide, Et_3N = triethylamine, c-pentane = cyclopentane, and c-hexane = cyclohexane. The product distribution was determined using ^{1}H-NMR in DMSO-d_6 using $DMSO_2$ as an external standard.

group increases. For DMSO, a higher conversion of *cc*MA was observed besides its lower polarity and aprotic properties. Similar activity was obtained with sulfolane solvent (owing sulfone groups). From the solvent screening, it is clear that solvent properties play an essential but multifaceted role in assisting the isomerization, given its effect cannot be ascribed to only basicity, polarity, or proticity.

Under the studied conditions, the formation of *tt*MA was not noticed, while Mlac was mainly formed in solvents promoting the first isomerization, except for DMSO, albeit in very little amounts in ethanol. These results suggest that lactonization becomes more favorable than the second isomerization, *viz*. *ct*MA to *tt*MA, in these solvents.[15] Due to their high *ct*MA yields in the first screening, water, ethanol, DMSO, and DMF solvents were selected to further investigate the tendency for lactonization *vs.* isomerization.

The parallel (Mlac ← *ct*MA → *tt*MA) reaction network in the selected solvents was investigated kinetically into more detail by varying the initial concentration of *ct*MA from 30 to 300 mM. *ct*MA was used as feedstock instead of *cc*MA to eliminate complexity due to the contribution of the first isomerization step. Interestingly, the formation of *tt*MA was not noticed in any of the conducted reactions, instead, Mlac was the only observed product (Fig. 2).

At 30 mM concentration, the amount of produced Mlac after 4 hours was higher in H_2O and DMF (11.5 mM and 7.0 mM, respectively) in comparison to EtOH (1.5 mM) and DMSO (no formation of Mlac). The possible involvement of acidic hydrogen from the solvent in favoring the formation of Mlac from *ct*MA was proposed by Tessonnier *et al.* according to the in water reported mechanism (Fig. S3†).[26] We believe that the basic nature of DMF can assist the formation of Mlac according to the same mechanism. Increasing the initial concentration of *ct*MA from 30 mM to 100 mM was followed by an increase in the formation rate of Mlac in H_2O (from 3.2 to 11.0 mM h^{-1}), DMF (from 1.8 to 5.6 mM h^{-1}), and EtOH (from 0.3 to 1.0 mM h^{-1}), pointing to the occurrence of an autocatalyzed lactonization mechanism of *ct*MA, as presented in Fig. S5.†[32] Only in DMSO, Mlac was not formed in the 100 mM solution, which can be explained by the effect of DMSO in increasing the pK_a of carboxylic acid groups, disfavoring Brønsted acid catalyzed mechanisms such as the acid-catalyzed intramolecular lactonization of *ct*MA in this case.[36] In addition, DMSO can stabilize *ct*MA by interacting with the C=C bonds, as shown later in the proposed reaction mechanism (Fig. 5B), which will likely lead to less Mlac formation. A further increase in the initial concentration of *ct*MA to 300 mM increases the formation rate of Mlac even more, as 28.4, 25.1, and 3.4 mM h^{-1} were measured in H_2O, DMF, and EtOH, respectively. At this concentration, around 9% of Mlac was formed after 4 hours in DMSO (7.0 mM h^{-1}). Enhanced Mlac formation at high concentrations of MA confirms that lactonization follows an acid-catalyzed pathway with MA, both reactant and catalyst, as reported in literature and illustrated in Fig. S5.†[15,32] Interestingly, by following the evolution of the Mlac productivity as a function of the initial concentration of *ct*MA, one may conclude a positive order of the lactonization reaction in *ct*MA (Fig. S6†). Remarkably, Mlac formation was only visible in DMSO in the 300 mM *ct*MA solution.

Upon an increase of the reaction temperature to 120 °C, the production of Mlac increased for all solvents (Fig. 3, 100 mM solution). The maximal Mlac yield was again obtained in H_2O and DMF, at 73 and 52 mM, respectively. The formation of dimuconolactone (Dlac) was also noticed in H_2O at 120 °C. Less Mlac formation was found in EtOH, while *tt*MA was only formed in DMSO, with a *tt*MA to Mlac ratio of 6.7. The absence of *tt*MA at 90 °C can be explained by the relatively short reaction time (4 hours), where Tessonnier *et al.* reported the need for around 50–60 hours to produce 20% at 87 °C, respectively.[32] This unique ability shows that DMSO selectively promotes the *ct*MA to *tt*MA isomerization, whereas other solvents (H_2O and DMF) are more efficient for the primary *cc*MA to *ct*MA isomerization.

In conclusion, this first screening clarified that the competitive lactonization reaction is boosted by several factors, including temperature, initial MA concentration (or acidity), and the solvent properties. The observations align with earlier reports, studying isomerization/lactonization of MA.[15,26,28] The second isomerization forming *tt*MA is kinetically hindered in all solvents, except in DMSO. The role of DMSO in *tt*MA formation may be ascribed either to an indirect (stabilization) effect, such as the stabilization of MA to prohibit the acid-cata-

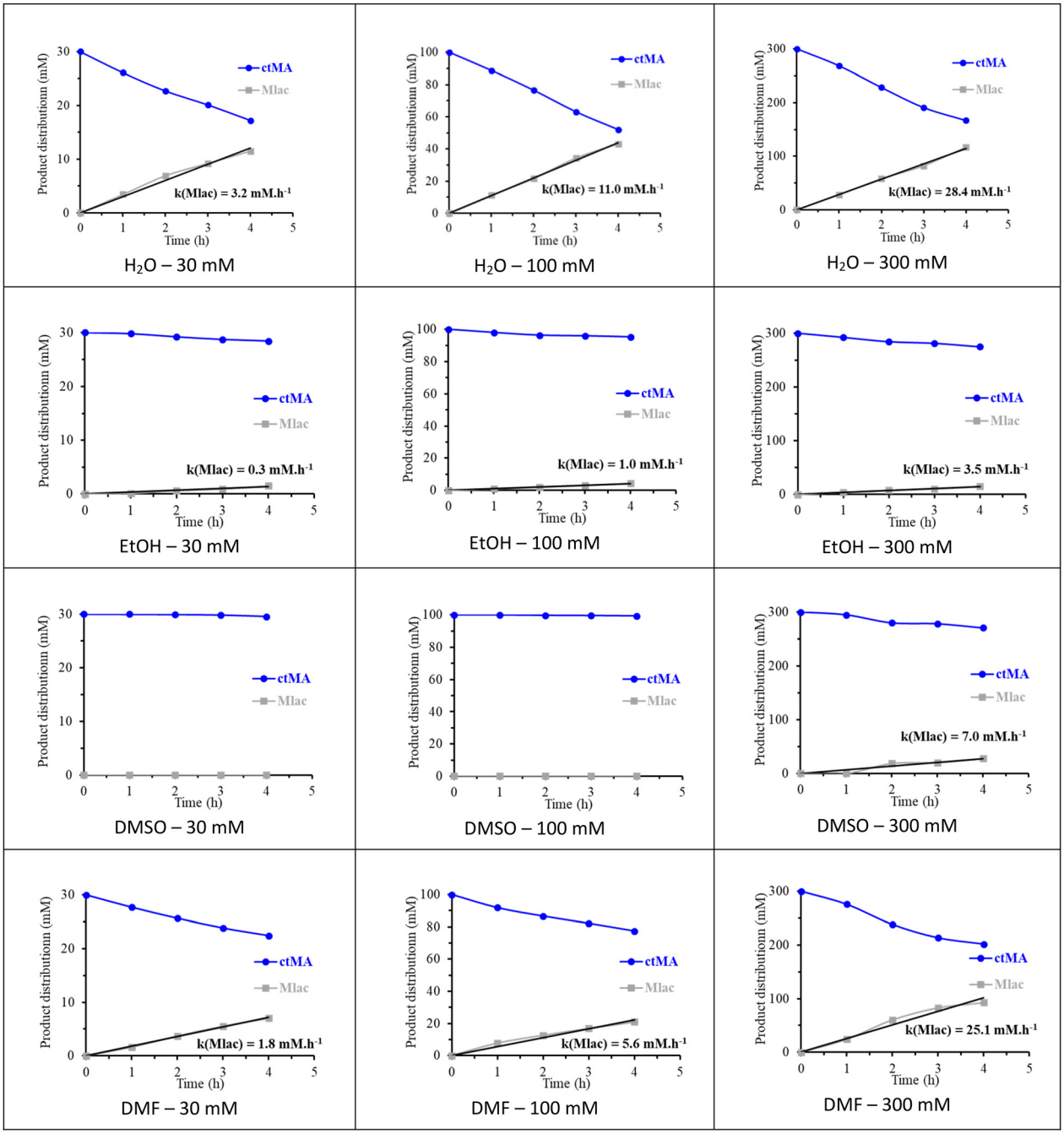

Fig. 2 The time profile of the conversion of *ct*MA (30, 100, and 300 mM) solutions in H_2O, EtOH, DMSO, and DMF solvents at 90 °C. The amount of remaining *ct*MA and produced Mlac is reported in mM. The formation of *tt*MA was- not noticed. The product distribution was determined using ^{1}H-NMR in DMSO-d_6 using $DMSO_2$ as an external standard.

lyzed intramolecular lactonization, or to its direct involvement in the reaction mechanism. However, this role is limited to low substrate concentration, given that Mlac formation is higher for more concentrated MA solutions.

Role of water on the reaction pathways

pH dependency and enhanced Mlac formation. Addition of water to DMSO lowers lactonization in favor of the selectivity to *tt*MA.[32] However, the optimal molar ratio for H_2O/MA varies somewhere between 0.9/1 and 10/1. Notably, we observed that an optimal ratio at a given MA concentration does not imply it being suitable for another concentration. When performing the reaction in the presence of 2 molar equivalents water (to MA) in a 100 mM solution of *ct*MA in DMSO, an increase in the ratio of produced *tt*MA to Mlac from around 0.3 (in absence of H_2O) to 5.1 (Fig. 4A and Table S1†) is found. At

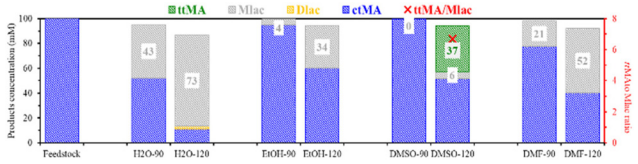

Fig. 3 The temperature effect on the product distribution (in mM) of the conversion of 100 mM *ct*MA in H_2O, EtOH, DMSO, and DMF at 90 and 120 °C after 4 hours. The product distribution was analyzed with quantitative ^{1}H-NMR analysis in DMSO-d_6 using $DMSO_2$ as an external standard.

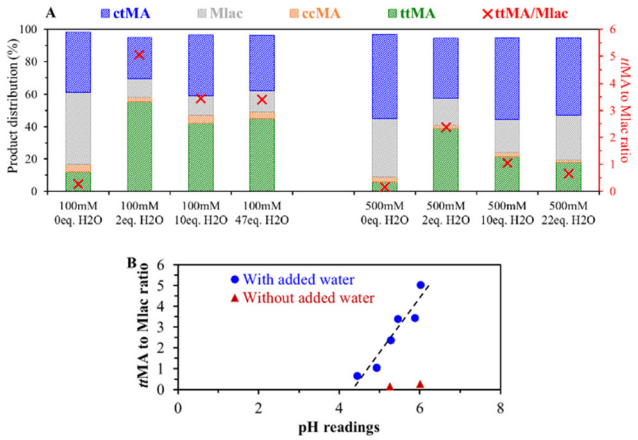

Fig. 4 (A) The product distribution of the isomerization of 100 and 500 mM *ct*MA in DMSO as a function of the amount of added water equivalents to MA. The reactions were performed in glass pressure tubes at 150 °C for 1 hour. The values of the *tt*MA to Mlac ratio are plotted on the right (red) *y*-axis. (B) Effect of the initial pH reading value on the obtained *tt*MA to Mlac molar ratio at the end of the isomerization reaction. The points in blue correspond to 6 reactions performed at initial 100 and 500 mM concentrations with added H_2O equivalents (see Fig. 4A). The red triangles show experiments without added water (0 eq. H_2O) at 100 and 500 mM initial concentration of *ct*MA.

10 molar equivalents of H_2O, this ratio drops to nearly 3.5, which remains at higher water equivalents (up to 47 eq.). To understand the reasons behind this drop, we followed the pH evolution in dry DMSO during the addition of *ct*MA and different H_2O equivalents (Fig. S7†). In absence of water addition, the conventional pH scale (from 0 to 14) is not applicable in organic solvents due to the unreliable measure of the H^+ concentration. Herein, a relative comparison of the pH reading is considered. A quick drop in the pH values, from 10.1 to 7.5, was observed after addition of the first 22 mM of *ct*MA (Fig. S7† and Fig. 4A). A lower effect on pH resulted from further increases in concentration, showing a pH of 6.0 at 100 mM. Then, controlled amounts of water are added to the solution from 0.5 to 47 equivalents relative to MA (Fig. S7† and Fig. 4B). Interestingly, little to no effect on the pH evolution was noticed up to 4–5 equivalents of H_2O, while the pH drops to 5.8 and 5.4 at 10 and 47 H_2O eq., respectively. The higher acidity of the solution favors Mlac formation, resulting in a lower *tt*MA to Mlac ratio. Additionally, the high initial concentration of *ct*MA also increased the acidity of the solution, reaching pH = 5.3 at 500 mM (Fig. S7C†). Therefore, a lower *tt*MA to Mlac ratio is obtained (Fig. 4A – 100 mM *vs.* 500 mM with 0 eq. H_2O). After adding 2 equivalents H_2O, the pH was maintained at around 5.0, while the *tt*MA to Mlac ratio climbed (Fig. 4A and Fig. S7D†). This points again to the beneficial role of water in the formation of *tt*MA. At higher H_2O equivalents (10 and 22 eq.), a drop in pH is noticed alongside a lower *tt*MA to Mlac ratio. A correlation between the pH readout values and the formation of Mlac can thus be established (Fig. 4B). The higher the acidity, the more Mlac is formed, and this translates to the use of low substrate concentration in the MA isomerization process to *tt*MA.

Mlac was the major side product and the only one quantified in this study due to its predominance over other side products. However, other side products still arose at high enough concentrations to allow their identification and they were formed in competition to isomerization. Due to their minor amounts, these products were not identified and are represented in the graphs as the loss in carbon balance (product distribution not reaching 100%). Their chemical structures, along with their chemical shifts for ^{1}H-NMR and ^{13}C-NMR, are shown in Fig. S8.† Beyond Mlac, the di-muconolactone form of MA (Dlac) was analyzed. In addition, a hydroxylated version of Mlac and some aldehyde species were present, likely a result of redox chemistry on the MA chain, as shown in Fig. S8.†

In our attempts to reduce the acid-catalyzed side reactions, including lactonization, we studied the effect of adding a base. Controlled additions of base, such as triethylamine, to reach pH around 6 (MA to triethylamine molar ratio of 17), lead to various degradation products. Similar results were obtained after the addition of alkaline salts, *e.g.*, $KHCO_3$. Also, no beneficial effect was noticed with weak organic bases such as pyridine and potassium thiocyanate, in contrast, their presence rather slows the *ct*MA to *tt*MA isomerization. Thus, higher pH does not necessarily recover a lost isomerization activity. We also noted that the trend between pH and Mlac formation does not extrapolate to the tests without added water (red triangles in Fig. 4B) and thus fails to explain the low *tt*MA to Mlac ratio in dry DMSO. The low *tt*MA to Mlac ratio in the absence of water, therefore, suggests the direct involvement of water in the isomerization.

Plausible reaction mechanism of the *ct*MA to *tt*MA isomerization. *In situ* monitoring of water was performed with ^{1}H-NMR during the conversion of *cc*MA to *ct*MA, and finally to *tt*MA. The evolution of water appearance over the course of the isomerization, displayed in Fig. 5A, is in line with the earlier work of Tessonnier *et al.*, who reported a gradual decrease in water signal upon conversion of *ct*MA.[32] Our data also shows the emerging of *tt*MA at the decrease of the water signal (Fig. 5A). The *in situ* NMR experiment of Fig. 5A visualizes this change in water-induced behavior which can be due to a change in the acid–base properties or to the dynamic participation of water in the isomerization mechanism.

In different contexts, a mechanism for the isomerization of double bonds, that are conjugated with carboxylic acid groups,

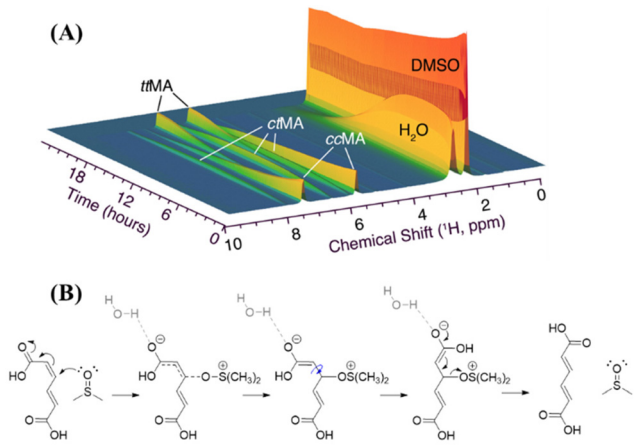

Fig. 5 (A) The evolution of the isomerization products of *cc*MA in DMSO as well as the water signal from *in situ* monitored ^{1}H-NMR measurements. (B) Plausible transient catalytic attack of DMSO on the C=C of MA followed by the rearrangement of the conjugated C=O functionality.

and involves a Michael-type addition of a nucleophile has been proposed.[37,38] While elaborating on this mechanism, we propose a plausible mechanism for the isomerization of MA in DMSO (Fig. 5B). This proposal is based on the unique molecular geometry of DMSO, which is characterized by a trigonal pyramidal-like structure with a highly polarized S–O single bond, in which the oxygen carries a partial negative and S a partial positive charge (Fig. S9†).[39] Therefore, DMSO can initiate a transient nucleophilic Michael addition *via* its nucleophilic oxygen atom on the C=C of MA, forming the corresponding enolate intermediate. Interestingly, in the conversion of *cc*MA to *tt*MA, some olefinic intermediates containing an alcoholic group next to the double bonds were observed in the real-time NMR spectra after the accumulation of *ct*MA. The signals of this intermediate in real-time NMR are marked with asterisks in Fig. S10.† Given the signals of the olefinic and sp^3 hybridized alcoholic groups evolve synchronically, they belong to the same intermediate molecule. This intermediate may be attributed to an adduct of a nucleophilic solvent addition on a double bond in MA. This enolate is stabilized by the presence of water. After the rotation of the C–C bond, *tt*MA is generated after the elimination of DMSO. The presence of the hydroxylated Mlac (Fig. S8†) indicates that the coordination of DMSO and the further hydrolysis of this coordination can occur. Among the side products formed in the reaction, enol forms that are stabilized through cyclization were identified. This indicates that DMSO/H_2O mixtures elicit a combined effect by increasing the pK_a value of MA while reducing lactonization and affording transient nucleophilic addition while stabilizing enol forms during isomerization.

Towards a selective and highly productive isomerization method

Counteracting lactonization: use of muconic ester. Counteracting the competitive lactonization is essential for selective *tt*MA formation in concentrated systems. This has been performed by several techniques, such as the use of lanthanum[26] or by esterification[28,31] (Fig. S11†). In this work, we prepared *cis*,*trans*-diethyl muconate (*ct*DEM), following the procedure reported in Ref. 31. Besides avoiding lactonization and increasing the selectivity towards the *tt*-isomer, muconic esters are highly soluble in organic solvents, while being a platform to produce poly-muconates, terephthalates, and adipates.[15,21,28]

The rate of the isomerization for both *ct*MA and *ct*DEM was first followed in DMSO at 120 °C, as shown in Fig. 6A and B. The two *ct*-isomers seem to react very analogously, judging from the reaction progress curves. This observation suggests a minor influence of deprotonation of the carboxylic groups in *ct* to *tt* isomerization, which is in line with our proposed mechanism (Fig. 5B). Importantly, as lactonization was successfully counteracted with DEM, high selectivity to its *tt*-isomer was achieved, *e.g.*, from 88% (*ct*MA → *tt*MA) to 100% (*ct*DEM → *tt*DEM) as shown in Fig. 5. *In situ* ^{1}H-NMR in DMSO-d_6 at 100 °C showed similar findings (Fig. S12†). The isomerization of *ct*DEM was further tested in the initial selection of solvents, including EtOH, DMSO, and DMF, but not H_2O due to the insolubility of DEM in H_2O. Even though the use of esters avoided Mlac formation in all solvents, *tt*DEM was only observed in DMSO, confirming its direct involvement in the isomerization mechanism.

Towards outstanding productivity. The isomerization of *ct*DEM in DMSO was further optimized to increase the volumetric productivity of the system (Table S2†). The optimization covers variations of the reaction temperature and initial concentration of *ct*DEM, as well as the controlled addition of other substrates in DMSO such as H_2O and $DMSO_2$.

At 100 mM *ct*DEM, the *tt*DEM yield increases rapidly with reaction temperature, from 5.8% in 24 hours at 80 °C to 76.4% in an hour at 150 °C (Table S2 entries 1–4† and Fig. 7), while maintaining a high selectivity towards *tt*DEM (>5%). All reactions were performed in the presence of 2 equivalents H_2O relative to *ct*DEM in DMSO. Due to the instability of DMSO with possible decomposition at higher temperatures, the temperature range was limited to 150 °C. For the same concentration, the absence of water reduces the formed *tt*DEM to

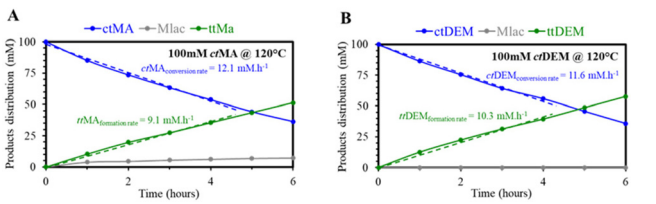

Fig. 6 The time profile of the isomerization of 100 mM *ct*MA and *ct*DEM in DMSO (5 mL) and 2eq. H_2O at 120 °C. The rate plots for the conversion of *ct*-isomer and the formation of the *tt*-isomer are obtained for the slope of the data points plotted between 0 and 4 hours. The reactions were performed in glass pressure tubes sealed under static conditions. The product distribution was determined by ^{1}H-NMR for the reaction in A and by GC for the reaction in B.

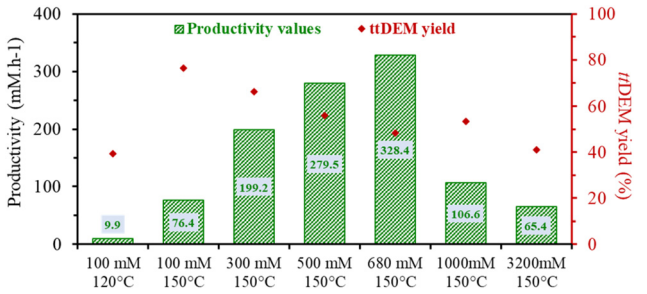

Fig. 7 A comparison of the increase in the productivity values as a function of the optimized reaction conditions. The values were selected for systems producing 40% or more of *tt*DEM. The yields of *tt*DEM corresponding to every productivity value are shown in red (right-hand *y*-axis).

18.3% (entry 5), while the presence of water between 2 and 20 equivalents left *tt*DEM yield unaltered (between 74% and 77%). Higher water equivalents retarded *tt*DEM formation to 47.1%, however, Mlac was not observed.

The addition of other reagents was also tested. As mentioned before the addition of organic base or alkaline salt was not beneficial to the isomerization, while degradation of muconates occurred. Methylphenyl sulfoxide (MPSO) was used as a sulfoxide-type solvent and co-solvent with DMSO, but *tt*DEM formation was not influenced, even slowed down for high MPSO contents (Table S2 – entries 10–15†). The isomerization activity vanished in pure MPSO solvent. We believe that this lower isomerization capacity of MPSO may result on the one hand from the lower polarization of its oxygen atom in comparison to DMSO, and the steric effect on the other hand. The addition of sulfones into DMSO was further tested, specifically sulfolane and dimethyl sulfone ($DMSO_2$). Sulfolane behaves like MPSO at low and high loadings (Table S2 – entries 16–20†). Interestingly, $DMSO_2$ beneficially affected the production of *tt*DEM (Table S2 – entries 21–23†). For a better visualization of the effect of $DMSO_2$, the isomerization was conducted at a lower temperature (120 °C) in the presence of 10 eq. $DMSO_2$ (Fig. S14†), and the results were compared to the ones obtained in the absence of $DMSO_2$ (Fig. 6B), showing a noticeable 10.3 to 13.7 mM h^{-1} increase in the *tt*DEM formation rate. Similar results were obtained with *in situ* NMR monitoring measurement for a solution of *cc*MA (Fig. S15†). The presence of $DMSO_2$ was also found to increase the conversion rate of *cc*MA in the first place by a factor of 1.2–1.3 (from 37% to 45% at 2.5 hours). The formation rate of *tt*MA, obtained from the second isomerization, increased by threefold at the 5 hours point.

Finally, the effect of increasing the initial concentration of *ct*DEM was tested (in presence of DMSO and 2 eq. H_2O at 150 °C). The progressive increase in the concentration led to higher productivity values of *tt*DEM where a maximum of 328.4 mM h^{-1} is obtained for an initial concentration of 680 mM h^{-1} (Table S3 – entry 6† and Fig. 7). The productivity drops at higher concentrations. A total selectivity towards *tt*DEM was noted up to 100 mM concentrated solutions and starts to drop at higher concentrations to reach around 95% between 500 and 2000 mM (Table S3†). The decrease in selectivity is mostly due to the reactivity of the *tt*-isomer in oligomerization reactions. However, contrary to *ct*MA, the increase in the amount of *ct*DEM does not reduce pH; pH varied only from 10 to 9.7 in the presence of 1000 mM *ct*DEM and 2000 mM H_2O. The non-acidic conditions enabled the *tt*-isomer formation, consistent with the absence of Mlac formation, even at concentrations as high as 1000 to 3200 mM (Table S3 – entries 7–9†).

Recovery of *tt*DEM. The high solubility of DMSO in water is a very important factor to consider in the isolation of *tt*DEM. Liquid extraction with a suitable organic solvent such as EtOAc was used here (for details see Materials and Methods). The extraction method was first applied to a series of parent solutions with different initial concentrations of *ct*DEM in the range of 30 to 500 mM (Fig. S16†). The recovery *r* was calculated according to the following formula: $r = [DEM]_{EtOAc}/[DEM]_{initial}$. For 30 mM concentration, the recovery level was modest ($r = 0.77$), however, this value further increased to around 0.95 in the range of 100–500 mM *ct*DEM. The ^{1}H-NMR purity of recovered *ct*DEM showed little to no remaining DMSO (Fig. S17†). The extraction of DEMs (*ct*DEM and *tt*DEM) from a series of post-reaction solutions was then investigated, showing high 0.88 to 0.94 recovery levels (Fig. 8). The highly concentrated solutions (1000 and 3200 mM) were diluted to around 500 mM prior to the recovery procedure. The produced *tt*DEM and unconverted *ct*DEM were thus both recovered in the EtOAc phase without a preferential removal affinity for a specific isomer, therefore maintaining almost the same isomeric *tt* to *ct* ratio from the isomerization reaction (red diamonds in Fig. 8). Once more, ^{1}H-NMR showed high purity of the EtOAc phase, demonstrating the efficiency of the procedure (Fig. S18†). The recovered DMSO in the aqueous phase can be re-used after extraction as solvent or reagent for additional reactions. Herein, after the water removal using reduced pressure and the further drying of DMSO (anhydrous magnesium sulfate), the recovered DMSO, from a 500 mM *ct*DEM + 2eq. H_2O reaction test, was tested in a new reaction cycle showing similar results in terms of *ct*DEM conversion and *tt*DEM yields (Fig. S19†).

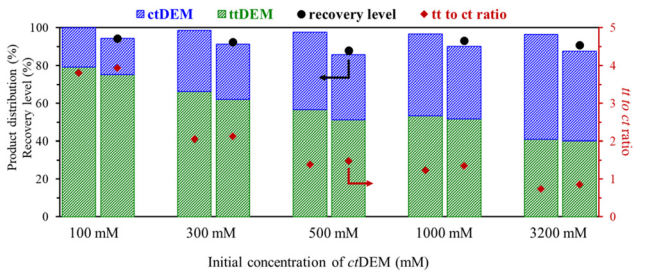

Fig. 8 The product distribution after isomerization and after extraction from DMSO. The recovery level (*r*) after extraction is plotted in black circle on a scale of 0 to 100% (left-hand *y*-axis). The ratio of *tt* to *ct* isomers was also calculated before and after the recovery and is plotted in red diamonds on the right-hand *y*-axis.

Sustainability of the isomerization methods: Green Chemistry principles

To assess the sustainable character of our isomerization method, we scored it along the principles of Green Chemistry and compared it to the best available isomerization practices in terms of *tt*-isomer productivity (Table S4†).[40–42] The solvent-driven isomerization method was compared to the most common reported isomerization method using homogeneous iodine catalysts. Seven of the twelve principles of green chemistry were selected and compared in Table S5.† The remaining five principles (designing safer chemicals, design for degradation, real-time analysis for pollution prevention, reduce derivatives, and inherently safer chemistry for accident prevention) are not considered relevant at this status of research. The details of the comparison and considered parameters can be found in the ESI (pages S12 and S13†).

The comparison between the isomerization methods revealed that iodine catalysis yields the highest *tt*MA (86%) and *tt*-muconates (95%) amounts. All the reactions show a high atom economy (AE), and they generally exhibit a low level of hazards, except for iodine catalysis, which uses toxic tetrahydrofuran (THF) and methanol (MeOH) as solvents. Also, iodine itself is a hazardous chemical and harmful to steel reactors. The need for the esterification of MA will affect both methods by increasing the waste production (*E*′-factor) and decreasing the atom economy (AE′), due to water formation from the esterification. However, this step was not considered due to its need either before or after the isomerization to access the high potential of these muconates, known for their high solubility and their use in polymerization as well as other chemical transformations (towards terephthalates and adipates).[15,21] Thus, with this consideration, all methods show a moderate *E*-factor (between 14.1 and 20.6), except for the isomerization of MA in DMSO (40.8) and the isomerization of DMM with iodine (41.8) (Table S5†). The main contributor to the high *E*-factor of the MA-in-DMSO method is the low yield of produced *tt*MA (40%), while the low initial concentration of di-methyl muconate (DMM = 118 mM) was the main contributor for DMM with iodine (Table S4†). Our new method (DEM-in-DMSO) resulted in an *E*-factor of 20.6, which is nearly half the *E*-factor of the same method using MA (40.8). Since the amount of solvent accounts for a very large part of the waste production, increasing the initial concentration of DEM will allow reducing the *E*-factor. By doubling the concentration of DEM (500 to 1000 mM), the *E*-factor will drop to nearly 11.3 at a production yield of 53.3% of *tt*DEM. This drop in waste production clearly stresses the high potential of the solvent-driven isomerization of muconic esters.

Conclusions

This work presents interesting solvent effects on the selective thermal isomerization of MA isomers and their esters (muconates). To avoid the competitive acid-catalyzed lactonization, use of esters in this isomerization chemistry is highly advised to be able to reach the highest isomer products selectivity. Whereas the primary *cc* to *ct* isomerization is less sensitive to the solvent properties, the *tt* isomer formation is only successful in DMSO with minor equivalents of water. A mechanism that explains the beneficial role of DMSO is proposed based on dedicated intermediate and side product analysis with real-time NMR. This mechanism considers direct nucleophilic addition chemistry, that promotes the subsequent *ct* to *tt* isomerization, while water plays a crucial role in stabilizing the intermediate adduct. High 328 mM h^{-1} *tt* isomer productivity with >95% selectivity can be achieved with this DMSO/H_2O solvent isomerization method after optimization of temperature and reagent concentration based on these mechanistic understandings. After isomerization of the muconates, the product isomers can be recovered almost quantitatively by extraction in ethyl acetate. A Green Chemistry principles analysis reveals a few promising metrics of the DMSO/H_2O method especially at high substrate/solvent ratios in highly concentrated reactions.

Author contributions

Ibrahim Khalil: conceptualization, investigation, methodology, funding acquisition, writing, review and editing. Fatima Rammal: investigation, methodology, review and editing. Lisa De Vriendt: investigation, review and editing. An Sofie Narmon: investigation, writing, review and editing. Bert Sels: resources, review and editing. Sebastian Meier: investigation, methodology, funding acquisition, resources, writing, review and editing. Michiel Dusselier: supervision, conceptualization, visualization, resources, funding acquisition, review and editing.

Conflicts of interest

There are no conflicts to declare.

Acknowledgements

I. Khalil acknowledges the FWO foundation for postdoctoral grants number 1260321N and 12A3M24N. Part of this work was performed in the framework of the Catalisti cluster SBO project SPICY ("Sugar-based chemicals and Polymers through Innovative Chemocatalysis and engineered Yeast"), with the financial support of VLAIO (Flemish Agency for Innovation and Entrepreneurship) (HBC.2017.0597). S. M acknowledges funding by the Independent Research Fund Denmark (grants 0217-00277A and 2035-00119B). The 800 MHz NMR spectra were recorded at the NMR Center DTU, supported by the Villum Foundation.

References

1 J.-P. Lange, *Nat. Catal.*, 2021, **4**, 186–192.
2 C. Zhou, I. Khalil, F. Rammal, M. Dusselier, P. Kumar, M. Lacroix, E. Makshina, Y. Liao and B. F. Sels, *ACS Catal.*, 2022, **12**, 11485–11493.

3 I. Bechthold, K. Bretz, S. Kabasci, R. Kopitzky and A. Springer, *Chem. Eng. Technol.*, 2008, **31**, 647–654.
4 F. Brandi, I. Khalil, M. Antonietti and M. Al-Naji, *ACS Sustainable Chem. Eng.*, 2021, **9**, 927–935.
5 M. A. Shah, I. Khalil, S. Tallarico, T. Donckels, P. Eloy, D. P. Debecker, M. Oliverio and M. Dusselier, *Dalton Trans.*, 2022, **51**, 10773–10778.
6 W. Schutyser, T. Renders, S. Van den Bosch, S.-F. Koelewijn, G. T. Beckham and B. F. Sels, *Chem. Soc. Rev.*, 2018, **47**, 852–908.
7 T. D. J. te Molder, S. R. A. Kersten, J.-P. Lange and M. P. Ruiz, *Ind. Eng. Chem. Res.*, 2021, **60**, 13515–13522.
8 F. Rammal, J. Matthijssen, I. Khalil, S. Calderon-Ardila, E. Makshina and B. F. Sels, *ACS Catal.*, 2023, **13**, 15811–15823.
9 Y. Liao, S.-F. Koelewijn, G. Van den Bossche, J. Van Aelst, S. Van den Bosch, T. Renders, K. Navare, T. Nicolaï, K. Van Aelst, M. Maesen, H. Matsushima, J. M. Thevelein, K. Van Acker, B. Lagrain, D. Verboekend and B. F. Sels, *Science*, 2020, **367**, 1385–1390.
10 M. Dusselier, P. Van Wouwe, A. Dewaele, E. Makshina and B. F. Sels, *Energy Environ. Sci.*, 2013, **6**, 1415.
11 N. A. Rorrer, J. R. Dorgan, D. R. Vardon, C. R. Martinez, Y. Yang and G. T. Beckham, *ACS Sustainable Chem. Eng.*, 2016, **4**, 6867–6876.
12 N. Z. Xie, H. Liang, R. B. Huang and P. Xu, *Biotechnol. Adv.*, 2014, **32**, 615–622.
13 B. Briou, B. Améduri and B. Boutevin, *Chem. Soc. Rev.*, 2021, **50**, 11055–11097.
14 B. H. Shanks and P. L. Keeling, *Green Chem.*, 2017, **19**, 3177–3185.
15 I. Khalil, G. Quintens, T. Junkers and M. Dusselier, *Green Chem.*, 2020, **22**, 1517–1541.
16 P. Carter, J. L. Trettin, T.-H. Lee, N. L. Chalgren, M. J. Forrester, B. H. Shanks, J.-P. Tessonnier and E. W. Cochran, *J. Am. Chem. Soc.*, 2022, **22**, 9548–9553.
17 C. Ling, G. L. Peabody, D. Salvachúa, Y.-M. Kim, C. M. Kneucker, C. H. Calvey, M. A. Monninger, N. M. Munoz, B. C. Poirier, K. J. Ramirez, P. C. St. John, S. P. Woodworth, J. K. Magnuson, K. E. Burnum-Johnson, A. M. Guss, C. W. Johnson and G. T. Beckham, *Nat. Commun.*, 2022, **13**, 4925.
18 J. E. Matthiesen, J. M. Carraher, M. Vasiliu, D. A. Dixon and J. P. Tessonnier, *ACS Sustainable Chem. Eng.*, 2016, **4**, 3575–3585.
19 S. Capelli, A. Rosengart, A. Villa, A. Citterio, A. Di Michele, C. L. Bianchi, L. Prati and C. Pirola, *Appl. Catal., B*, 2017, **218**, 220–229.
20 S. Capelli, D. Motta, C. Evangelisti, N. Dimitratos, L. Prati, C. Pirola and A. Villa, *ChemCatChem*, 2019, **11**, 3075–3084.
21 G. Quintens, J. Vrijsen, P. Adriaensens, D. Vanderzande and T. Junkers, *Polym. Chem.*, 2019, **40**, 5555–5563.
22 K. A. Curran, J. M. Leavitt, A. S. Karim and H. S. Alper, *Metab. Eng.*, 2013, **15**, 55–66.
23 C. W. Johnson, D. Salvachúa, P. Khanna, H. Smith, D. J. Peterson and G. T. Beckham, *Metab. Eng. Commun.*, 2016, **3**, 111–119.
24 D. R. Vardon, N. A. Rorrer, D. Salvachúa, A. E. Settle, C. W. Johnson, M. J. Menart, N. S. Cleveland, P. N. Ciesielski, K. X. Steirer, J. R. Dorgan and G. T. Beckham, *Green Chem.*, 2016, **18**, 3397–3413.
25 T. Nicolaï, Q. Deparis, M. R. Foulquié-Moreno and J. M. Thevelein, *Microb. Cell Fact.*, 2021, **20**, 114.
26 J. M. Carraher, T. Pfennig, R. G. Rao, B. H. Shanks and J. P. Tessonnier, *Green Chem.*, 2017, **19**, 3042–3050.
27 M. Shiramizu and F. D. Toste, *Angew. Chem., Int. Ed.*, 2013, **52**, 12905–12909.
28 A. E. Settle, L. Berstis, S. Zhang, N. A. Rorrer, H. Hu, R. M. Richards, G. T. Beckham, M. F. Crowley and D. R. Vardon, *ChemSusChem*, 2018, **11**, 1768–1780.
29 J. W. Frost, A. Miermont, D. Schweitzer and V. Bui, *US Patent*, US8426639B2, 2013.
30 V. Bui, D. MacRae and D. Schweitzer, *US Patent*, US8809583, 2014.
31 I. Khalil, M. G. Rigamonti, K. Janssens, A. Bugaev, T. Donckels, S. Robijns, D. De Vos and M. Dusselier, Single-Atom Ru-zeolite isomerization catalysis for a bio-based route towards terephthalates from muconic acid, 16 August 2022, PREPRINT (Version 1) available at Research Square.
32 J. M. Carraher, P. Carter, R. G. Rao, M. J. Forrester, T. Pfennig, B. H. Shanks, E. W. Cochran and J.-P. Tessonnier, *Green Chem.*, 2020, **22**, 6444–6454.
33 A. A. Turkin, F. Rammal, S. Eyley, W. Thielemans, E. V. Makshina and B. F. Sels, *ACS Sustainable Chem. Eng.*, 2023, **11**, 8968–8977.
34 J. M. Carraher, J. E. Matthiesen and J. P. Tessonnier, *J. Mol. Liq.*, 2016, **224**, 420–422.
35 J. W. Frost and K. M. Draths, *US Patent*, US5616496, 1997.
36 E. Rossini, A. D. Bochevarov and E. W. Knapp, *ACS Omega*, 2018, **3**, 1653–1662.
37 N. Hayama, Y. Kobayashi and Y. Takemoto, *Tetrahedron*, 2021, **89**, 132089.
38 M. F. Baruch, J. E. Pander, J. L. White and A. B. Bocarsly, *ACS Catal.*, 2015, **5**, 3148–3156.
39 Y.-C. Wen, H.-C. Kuo and H.-W. Jia, *J. Mol. Struct.*, 2016, **1109**, 154–160.
40 A. S. Narmon, E. Leys, I. Khalil, G. Ivanushkin and M. Dusselier, *Green Chem.*, 2022, **24**, 9709–9720.
41 S. Y. Tang, R. A. Bourne, R. L. Smith and M. Poliakoff, *Green Chem.*, 2008, **10**, 268–269.
42 P. T. Anastas and M. M. Kirchhoff, *Acc. Chem. Res.*, 2002, **35**, 686–694.